Crystalline structures of Rb_2UBr_6 ionic conductor determined by neutron diffraction

Krzysztof Maletka, E. Ressouche, Hakan Rundlof, Rolland Tellgren, Wlodzimierz Szczepaniak, Monika Zablocka-Malicka

NUKLEONIKA 2020;65(1):3–11
doi: 10.2478/nuka-2020-0001

ORIGINAL PAPER

Crystalline structures of Rb_2UBr_6 ionic conductor determined by neutron diffraction

Krzysztof Małetka, Eric Ressouche, Hakan Rundlof, Rolland Tellgren, Włodzimierz Szczepaniak, Monika Zabłocka-Malicka

Abstract. The neutron powder diffraction technique has been used for structural studies of Rb_2UBr_6 solid electrolyte as a function of temperature. The low-, room-, and high-temperature structures have been determined. At the temperature range of 4.2–80 K, the compound crystallizes in a monoclinic unit cell in the P21/c space group. At 80 K and 853 K, the compound crystallizes in a tetragonal unit cell in the P4/mnc space group. At 300 K, the lattice constants are a = b = 7.745(1) and c = 11.064(1) Å. At the temperature range of 853–960 K, a trigonal phase is observed in the $P\bar{3}ml$ space group.

Keywords: Neutron diffraction • Ionic conductivity • Solid electrolyte • Phase transitions • Crystalline structure • Uranium bromide

K. Małetka✉
National Centre for Nuclear Research
Radioisotope Centre POLATOM
Andrzeja Sołtana 7, 05-400 Otwock, Poland
E-mail: krzysztof.maletka@polatom.pl

E. Ressouche
Université Grenoble Alpes
CEA, IRIG, MEM, MDN
F-38000 Grenoble, France

H. Rundlof, R. Tellgren
Department of Inorganic Chemistry
Ángström Laboratory
Uppsala University
Box 538, S-75I 21 Uppsala, Sweden

W. Szczepaniak
Faculty of Environmental Engineering
Wrocław University of Science and Technology
Wybrzeże Wyspiańskiego 27, 50-370 Wrocław, Poland

M. Zabłocka-Malicka
Faculty of Chemistry
Wrocław University of Science and Technology
Wybrzeże Wyspiańskiego 27, 50-370 Wrocław, Poland

Received: 1 July 2019
Accepted: 30 October 2019

Introduction

Fast-ion conductors belong to the specific class of solids in which the regularity of the crystal lattices is significantly disrupted and are characterized by an almost liquid-like mobility of one of constituent ion species. Crystals with superionic phase at high temperatures approach this phase either gradually or through several phase transitions.

The group of uranium halides Me_2UX_6 (Me = Li, Na, ..., Cs; X = Cl, Br, I) forms a series of interesting compounds with closely related structures and exhibits several interesting properties such as peculiar sequences of structural phase transitions and fast ionic conductivity at elevated temperatures. The neutron diffraction studies were performed on a series of alkali uranium hexabromide and hexaiodide Me_2UX_6 (Me = Li, Na, Rb, X = Cl, Br, I) [1–9]. In spite of similar chemical formula, the Me_2UX_6 compounds exhibit a variety of thermodynamic and structural properties. Some of them (cf.: Cs_2UI_6 [10]) show large discontinuities in ionic conductivity only at the melting point with a low or moderate conductivity that increases gradually with temperature without any discontinuous change. The change from low to high ionic conductivity is spread over a wide range of temperatures, and these compounds do not exhibit any structural transformations. There is also a distinct group of compounds showing a large discontinuous change in ionic conductivity accompanied by a change in the lattice symmetry of both mobile and immobile sublattices (cf.: Na_2UBr_6, Na_2UI_6). Apart

from these two well-distinguished groups, it has been found that there are in addition such compounds in which ionic conductivity increases rather smoothly with temperature, but they do exhibit a change in lattice symmetry. A typical example of such a behaviour is Rb_2UBr_6. Its electrical conductivity has been measured by Szczepaniak [11], and it showed only an abrupt change at the melting point T_m = 997 K. At the whole temperature range below 997 K, the electrical conductivity changed in a continuous way although some irregularity on the ln(σT) vs. T^{-1} can be distinguished [11]. It was interpreted as an effect of small departure from stoichiometry (excess of RbBr) since the temperature where this irregularity occurred corresponded to the melting point of the eutectic phase RbBr–Rb_2UBr_6. On the other hand in the differential thermal analysis (DTA) curve of the rubidium hexabromouranate(IV), two possible structural transitions at 843 K and 967 K were found [11, 12]. In this paper, the specific structural properties of Rb_2UBr_6 compounds are reviewed and their influence on electrical conductivity are discussed.

Experimental

The samples were prepared as described earlier [1, 13]. The low temperature parts of experiments were performed using a powder sample of Rb_2UBr_6 sealed in a cylindrical thin-walled vanadium can of 10 mm diameter in a glove box under a dry argon atmosphere.

The measurements at room temperature were performed at the EWA reactor in the Institute of Atomic Energy, Świerk, using the TKSN 200 diffractometer and then repeated at the SILOE reactor in the Grenoble's Centre des Etudes Nucléaires (CENG) using the DN-5 diffractometer. The low temperature measurements were also performed in the CENG. Neutron powder diffraction patterns were taken using an "orange" cryostat at temperatures 300 K, during slow cooling down in the temperature range of 300–4.2 K, and at 4.2 K.

The high temperature experiments were performed at the Studsvik Neutron Research Laboratory (NFL) on the SLAD and NPD neutron powder diffraction instruments. In these experiments, the samples of Rb_2UBr_6 sealed in a thin-walled quartz tube of 6- and 12-mm diameter were used, respectively, for SLAD and NPD instruments. The sample used on the NPD was a polycrystalline, whereas that on the SLAD was a powder one [14].

For the Rietveld refinement, the program FullProf was used [15].

The room temperature structure of Rb_2UBr_6

Vdovenko *et al*. basing on the X-ray study have reported the Rb_2UBr_6 compound to crystallizes in the cubic system with the unit cell constant a = 10.94 Å, space group $Fm\bar{3}m$ with the K_2PtCl_6 type structure. No structural phase transitions were reported [1].

Our initial measurements at room temperature were performed at the EWA reactor in the Institute of Atomic Energy, Świerk, Poland. The measurement performed on the low-resolution TKSN 200 diffractometer of neutron wavelength λ = 1.56 Å showed close resemblance with the mentioned structure but also indicated that the assignment of $Fm\bar{3}m$ space group was wrong since apart from those peaks that eventually could be assigned to the $Fm\bar{3}m$ space group (general extinction rule: h+k, k+l, h+l = 2n), there appeared peaks (310) and (321) with h, k, l not satisfying this condition (cf.: Fig. 1). The result obtained so far however allowed to assign the structure to the cubic system with the unit cell constants close to those given by Vdovenko. Therefore, we searched solution of the structure in the frame of space groups that allowed the existence of additional reflections. These space groups were Pn3m, Pm3n, Pn3n, Pm3m, $P\bar{4}3n$, $P\bar{4}3m$, P4132, P4332, P4232, P432, Pn3, Pm3, P213, and P23. The Rietveld refinements performed for each of them have shown however that the satisfying solution of the structure in the cubic system cannot be achieved.

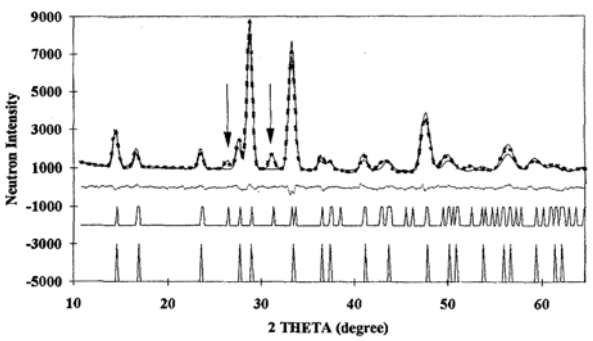

Fig. 1. Observed (points) and calculated in the cubic structure of K_2PtCl_6 type and in the tetragonal system, (lines) neutron diffraction patterns of Rb_2UBr_6 obtained at 300 K on the TKSN 200 diffractometer in Świerk. The curve at the bottom of the diagram shows the difference $I_{obs} - I_{calc}$ of the tetragonal system. The cubic (down) and tetragonal (up) peak positions are marked by vertical lines. The additional reflections forbidden in the K_2PtCl_6 type of structure are marked by arrows.

We concluded that the symmetry of the structure is lower and the structure should be described in other than the cubic crystallographic system. However, this should result in splitting of some diffraction lines, which should be seen on the diffraction data. The lack of this effect on our diffraction data could be caused by the lower resolution of used diffractometers, and for determination of the structure, the measurement on the diffractometer with a much better resolution is necessary. This measurement was performed on the DN5 diffractometer in the CENG.

The DN5 diffractometer was placed in the SILOE reactor. This instrument was a two-axis diffractometer with a medium resolution. The DN5 diffractometer used a BF3 position-sensitive "banana" detector of 800 cells. Diffraction data were collected in 2Φ steps of 0.1° over the range of 3–80°. During the measurement, a neutron wavelength of 2.48 Å was used for better separation of diffraction lines. The neutron diagram obtained at room temperature is shown in Fig. 2.

The obtained result of the experiment shows clearly that at room temperature, the expected

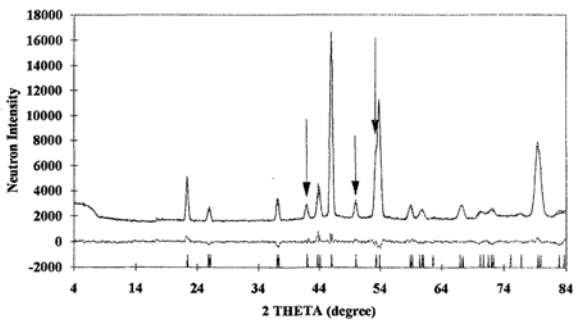

Fig. 2. Observed (points) and calculated (lines) neutron diffraction patterns of Rb_2UBr_6 obtained at 300 K on the DN5 diffractometer. The curve at the bottom of the diagram is the difference $I_{obs} - I_{calc}$. The peak positions are marked by vertical lines. The additional reflections forbidden in the cubic K_2PtCl_6 type of structure are marked by arrows.

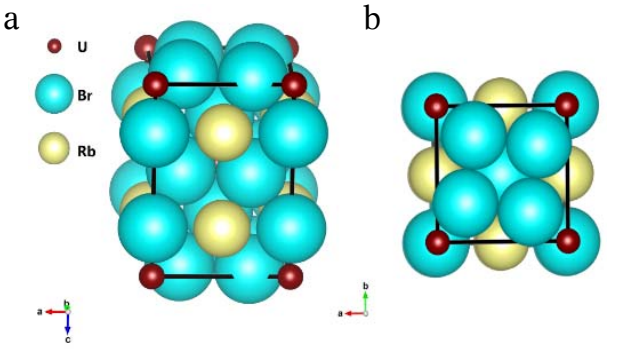

Fig. 3. The room temperature structure of Rb_2UBr_6. (a) View along the b axis of the tetragonal P4/mnc unit cell. (b) View along the c axis.

splitting of some diffraction lines really occurs. A special effect of this is seen on the cubic 004 type of reflection.

The first problem was to identify the true lattice constants and possible space groups. We found that all peaks were satisfactorily indexed in the tetragonal system with the unit cell constants $a_{tetr} = b_{tetr} = 7.739(3)$ and $c_{tetr} = 11.056(3)$ Å. The new lattice constants can be derived from those of the cubic by a slight expansion of one edge. The relation between the appropriate tetragonal and cubic lattice constants is $a_{tetr} \approx a_{cub}/\sqrt{2}$ and $c_{tetr} \approx a_{cub}$. This relation shows that in the tetragonal unit cell, two uranium ions occupy (0,0,0) and (1/2,1/2,1/2) positions. The four rubidium ions should be placed in positions with atomic coordinates close to ±(0.5, 0.0, 0.25) and ±(0.0, 0.5, 0.25). The twelve bromine ions have to form the octahedral and dodecahedral environment of uranium and rubidium ions.

The inspections of neutron diagrams showed that the reflections of hkl and hk0 types are not related. The diffraction lines of type 0kl and hhl fill up the extinction rules 0kl: k + l = 2n and hhl: l = 2n. These conditions limited the set of possible space groups into groups: P42/mnm, P42/mmc, P4/mnc, and P4/mmm. The P42/mnm may get eliminated at once because U ions would have to be placed in (0,0,0) and (0,0,1/2) positions. The solution of the structure for the remaining space groups was searched using a Rietveld profile analysis. We found that additional lines appeared only for the P4/mnc space group. In this solution of the structure, the agreement factors were also the best. The final results of calculations are presented in Table 1.

The atomic coordinates of Br ions show that the additional lines appearing on the neutron diagram at 300 K came from the deformation of K_2PtCl_6-type structure by coil up of the UBr_6^{-2} octahedrons and deformation of dodecahedral environment of Rb ions. The view of the structure is presented in Fig. 3.

The low temperature structure of Rb_2UBr_6

In order to check the stability of this structure in a wider range of temperatures and to make the noticeable effect of lattice vibrations damped, the measurements were also carried out at 4.2 K.

Neutron powder diffraction patterns were taken using an "orange" cryostat at temperatures 300 K, during a slow cooling down in the temperature range of 300–4.2 K, and at 4.2 K. During the cooling down, the diffraction data were also noted. With decrease in temperature, it was noticed that the diffraction pattern at 80 K has apparently changed and the pattern was stable up to 4.2 K. The neutron diagram observed at 4.2 K is shown in Fig. 4.

Splitting of the cubic 004 reflection observed previously at room temperature indicates that a tetragonal deformation has vanished completely.

Table 1. Rb_2UBr_6 at T = 300 K, space group P4/mnc, unit cell constant: a = b = 7.745(1), c = 11.064(1) Å

Name	Position	x	y	z	B	Occurrence
U	2a	0	0	0	0.8(3)	1
Rb	4d	0	1/2	1/4	6.8(4)	1
Br_1	8h	0.784(1)	0.286(1)	0	4.7(5)	1
Br_2	4e	0	0	0.252(1)	4.7(5)	1
			Distance [Å]			
U–Br		×4			2.776(8)	
U–Br		×2			2.788(1)	
Rb–Br		×4			3.873(5)	
Rb–Br		×4			3.633(3)	
Rb–Br		×4			4.171(3)	

Reliability factors:
Least-squares refinement – Rp: 3.2, Rwp: 4.2, Rexp: 2.0, χ^2: 4.7.
Conventional Rietveld R-factors – Rp: 11.4, Rwp: 10.3, Rexp: 4.7, χ^2: 4 7.

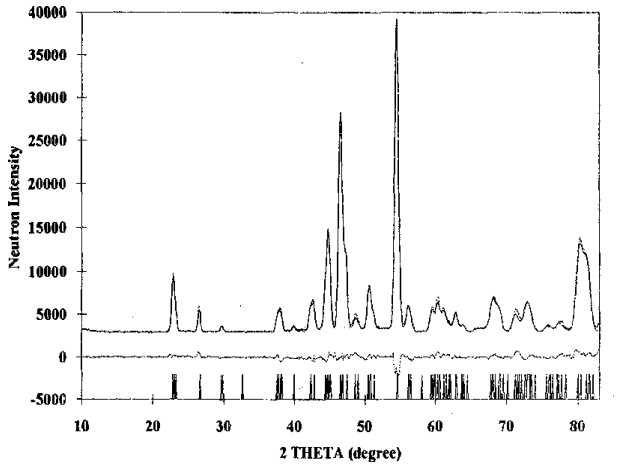

Fig. 4. Observed (points) and calculated (lines) neutron diffraction patterns of Rb_2UBr_6 obtained at 4.2 K on the DN5 diffractometer. The curve at the bottom of the diagram is the difference $I_{obs} - I_{calc}$. The peak positions are marked by vertical lines.

Instead, we observed a new deformation manifested by a splitting of the 202 line and the appearance of new weak peaks. It suggested that the orthorhombic deformation of the lattice occurs at 80 K especially since the indexation of neutron diagram at 4.2 K yields the orthorhombic unit cell constants a_{rhom} = 7.62, b_{rhom} = 7.77, and c_{rhom} = 10.87 Å. We searched solution of the structure with the possible space groups Pnma, Pmna, Pmma, and Pmmm and two noncentrosymmetric space groups Pmm2 and P222 using a Rietveld profile analysis. However, no correct solutions were found. Such a result suggested the existence of monoclinic distortion.

The monoclinic unit cell with the volume close to the volume of tetragonal cell can be implemented in two ways:

– by a slight compression and expansion of the corresponding tetragonal edges, and a small departure of the β angle from 90°. Therefore $a_{mon} \approx a_{tetr}$, $b_{mon} \approx a_{tetr}$, and $c_{mon} \approx c_{tetr}$;
– as is visualized in Fig. 10. The new unit cells may be derived from pseudo-tetragonal unit cell constants by the following relations: $a \approx a_{tetr}$, $b \approx a_{tetr}$, $c \approx \sqrt{(a_{tetr}^2 + c_{tetr}^2)}$ and $\beta \approx 124°$.

We assumed the centrosymmetric solution of the structure.

In the first case of the monoclinic system, the extinction rule h0l: l = 2n was found from the analysis of observed reflections. The rule limited the searches of solution of the crystal structure into P2/c, P21/m, and P2/m space groups. The P2/c and P21/m space groups were excluded at once because uranium ions would have to occupy (2a) position with coordinates (0,0,0), (0,0,1/2) and (0,0,0), and $(0, 1/2, 0)$, respectively. This yields a great difference between observed and calculated profiles. The calculation performed with the P2/m space group was unsuccessful. The reliability factors were Rp: 9.0, Rwp: 13.1, Rexp: 1.4, χ^2: 90.0 for least-squares refinement and Rp: 22.6, Rwp: 26.0, Rexp: 2.7, χ^2: 90.0 for conventional Rietveld R-factors. Furthermore, on the calculated spectrum appeared the lines 001, 010, and 100, which were not observed on the experimental profile. Hence, we concluded that in this space group, the solution of the structure did not exist.

In the second case of monoclinic unit cell, the observed indices of type hkl have not revealed any extra conditions, whereas the diffraction lines of type h0l and 0k0 satisfy the rules: h0l; l = 2n and 0k0; k = 2n. This extinction rules yield the monoclinic P21/c or P2/c space groups. With only P21/c space group however, the uranium ions could occupy (2a) position with the atomic coordinates (0,0,0) and $(0, 1/2, 1/2)$. This position is equivalent to (0,0,0) and $(1/2, 1/2, 1/2)$ positions of the tetragonal unit cell. These circumstances show that the solution of structure could exist just in the P21/c space group. The Rietveld profile refinement performed with this space group yields satisfactory factors of agreements with atomic parameters shown in Table 2.

Table 2. Rb_2UBr_6 at T = 4.2 K, space group P21/c, unit cell constant: a = 7.637(1), b = 7.767(1), c = 13.232(2) Å, β = 124.61(1) deg

Name	Position	x	y	z	B	Occurrence
U	2a	0	0	0	0	1
Rb	4e	–0.742(2)	0.049(8)	–0.247(1)	0	1
Br_1	4e	0.321(2)	0.209(2)	0.034(1)	0	1
Br_2	4e	0.220(2)	0.716(1)	0.024(9)	0	1
Br_3	4e	–0.790(2)	–0.503(9)	–0.239(1)	0	1
			Distance [Å]			
U–Br		×2		2.680(8)		
U–Br		×2		2.866(6)		
U–Br		×2		2.755(3)		
Rb–Br		×2		3.508(5)		
Rb–Br		×2		3.685(8)		
Rb–Br		×2		3.464(1)		
Rb–Br		×2		3.706(4)		
Rb–Br		×2		3.816(6)		
Rb–Br		×2		3.535(9)		

Reliability factors:
Least-squares refinement – Rp: 3.6, Rwp: 4.6, Rexp: 1.4, χ^2: 12.3.
Conventional Rietveld R-factors – Rp: 9.1, Rwp: 9.4, Rexp: 2.7, χ^2: 12.3.

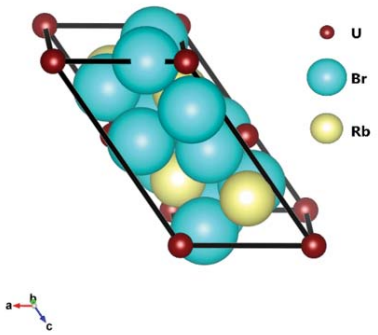

Fig. 5. The structure of Rb_2UBr_6 at 4.2 K.

This result allowed to approve that the low temperature structure of Rb_2UBr_6 has been determined. The view of the structure is shown in Fig. 5.

The high temperature structures of Rb_2UBr_6

The dependence of electrical conductivity and the results of differential thermal analysis (DTA) as well as data envelopment analysis (DEA) measurements were shown in the works of Refs. [10, 11]. The thermal data revealed that at 843 K and 967 K, the phase transitions may occur. On the temperature dependence of conductivity, the high rising of conductivity was registered at the temperature region of 740–870 K. Above 870 K, the arising of conductivity is much smaller. The curve is smooth. There were no indicated jumps typical for phase transition of the first order (Fig. 6).

To describe the structures at elevated temperatures, a neutron diffraction experiment was performed at 300, 600, 850, 900, 940, and 980 K on the SLAD instrument.

The SLAD instrument was a two-axis diffractometer with a medium resolution utilizing three banks of position-sensitive detectors that produced a diffraction spectrum in the range of 4–137° with a step of 0.1°. A vertically focusing monochromator with an incident neutron wavelength of 1.113(1) was used throughout the experiment. The non-linear background coming from a quartz tube was eliminated by subtracting the measured neutron diffraction profile for an empty quartz container. In experiments performed at elevated temperatures, a furnace with a tantalum heating element with automatic temperature control was used. The data were corrected for background scattering, container scattering, absorption, and inelastic and multiple scattering and normalized to a vanadium standard using the correct program package.

The neutron data at 600, 850, 900, 940, and 980 K are shown in Fig. 7.

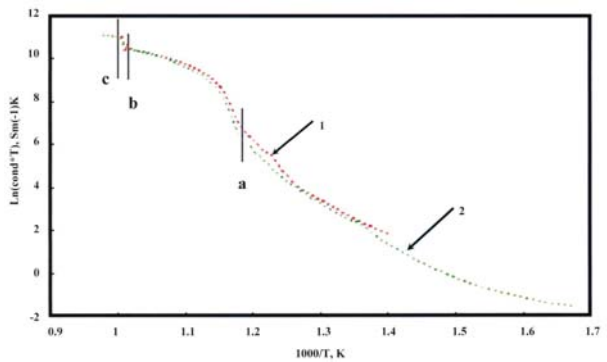

Fig. 6. Electrical conductivity of Rb_2UBr_6. (a) Beginning of the DTA effect of phase transition (?) at 843 K, (b) DTA effect of phase transition (?) at 967 K, and (c) melting, 997 K [11]. 1 – heating and 2 – cooling.

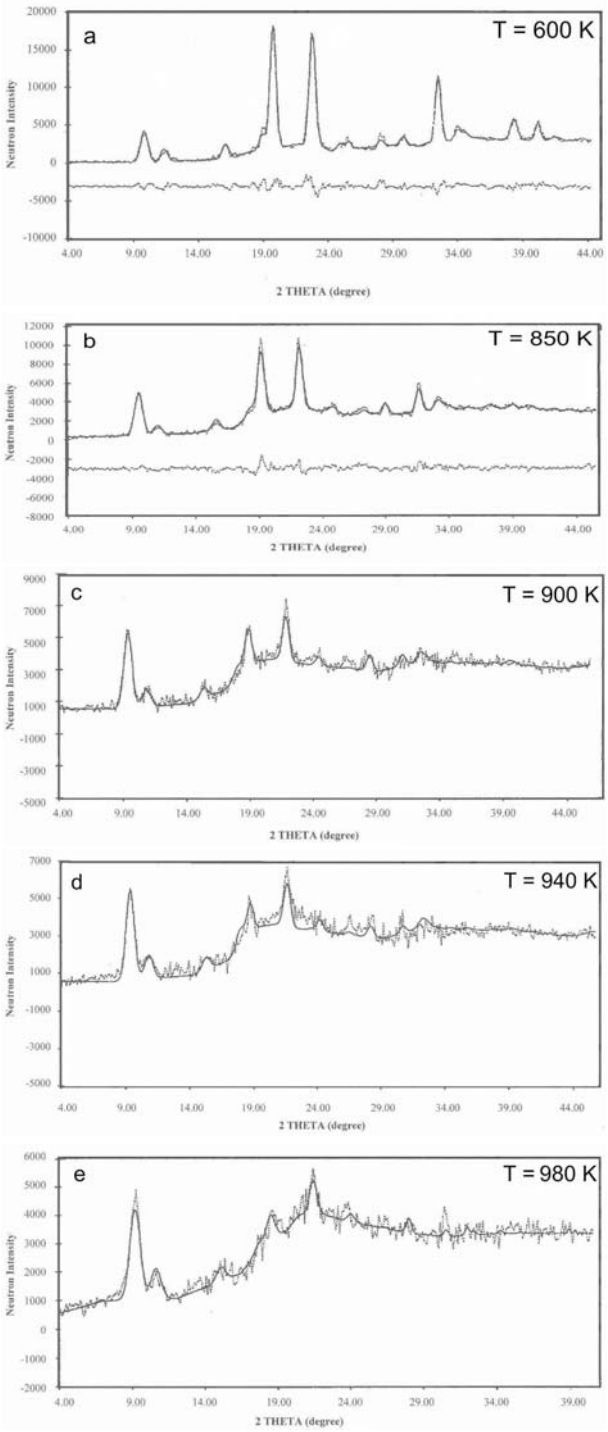

Fig. 7. Observed (points) and calculated (lines) neutron diffraction patterns of Rb_2UBr_6 obtained at 600, 850, 900, 940, and 980 K on the SLAD diffractometer. The curves at the bottom of each diagram are the differences $I_{obs} - I_{calc}$. In (a) and (b), the fitting of tetragonal structure is shown, whereas other presents the fitting of cubic structure. The peak positions are marked by vertical lines.

Table 3. Rb_2UBr_6 at T = 600 K, space group P4/mnc, unit cell constant: a = b = 7.960(4), c = 11.153(8) Å

Name	Position	x	y	z	B	Occurrence
U	2a	0	0	0	6.5(5)	1
Rb	4d	0	1/2	1/4	11.8(6)	1
Br_1	8h	0.749(4)	0.235(4)	0	10.8(4)	1
Br_2	4e	0	0	0.250(5)	10.8(4)	1
			Distance [Å]			
U–Br			×4		2.737(9)	
U–Br			×2		2.788(3)	
Rb–Br			×4		3.980(1)	
Rb–Br			×4		3.899(9)	
Rb–Br			×4		4.027(8)	

Reliability factors:
Least-squares refinement – Rp: 7.5, Rwp: 10.7, Rexp: 1. 8, χ^2: 36.7.
Conventional Rietveld R-factors – Rp: 21.6, Rwp: 21.9, Rexp: 3.6, χ^2: 36.7.

Table 4. Rb_2UBr_6 at T = 850 K, space group P4/mnc, unit cell constant: a = b = 8.15(2), c = 11.54(5) Å

Name	Position	x	y	z	B	Occurrence
U	2a	0	0	0	10(1)	1
Rb	4d	0	1/2	1/4	20(6)	1
Br_1	8h	0.75(1)	0.22(2)	0	18(4)	1
Br_2	4e	0	0	0.23(2)	18(4)	1

Reliability factors:
Least-squares refinement – Rp: 6.1, Rwp: 8.2, Rexp: 1.8, χ^2: 20.2.
Conventional Rietveld R-factors – Rp: 33.1, Rwp: 26.2, Rexp: 35.8, χ^2: 20.2.

Table 5. Rb_2UBr_6 space group $Fm\bar{3}m$, U in position (4a), Rb in position (8c), Br in position (24e)

T [K]	a [Å]	x_{Br}	B_U	B_{Rb}	B_{Br}	Occurrence of (8c)	Occurrence of (4b)
900	11.76(2)	0.212(4)	12(2)	36(4)	23(3)	0.96(3)	0.08(3)
940	11.91(3)	0.210(5)	13(3)	42(6)	30(2)	0.91(3)	0.19(3)
980	11.92(3)	0.210(7)	14(4)	54(6)	34(8)	0.96(3)	0.12(2)

Reliability factors:
– for T = 900 K: Least-squares refinement – Rp: 8.3, Rwp: 12.2, Rexp: 1.8, χ^2: 46.1. Conventional Rietveld R-factors – Rp: 65.2, Rwp: 50, Rexp: 7.3, χ^2: 46.1.
– for T = 940 K: Least-squares refinement – Rp: 8.2, Rwp: 11.3, Rexp: 1.8, χ^2: 39.2. Conventional Rietveld R-factors – Rp: 82, Rwp: 48, Rexp: 7.7, χ^2: 39.2.
– for T = 980 K: Least-squares refinement – Rp: 7.2, Rwp: 9.3, Rexp: 1.8, χ^2: 27.8. Conventional Rietveld R-factors – Rp: 95, Rwp: 51, Rexp: 10.0, χ^2: 27.8.

The DTA data show that up to 843 K, the crystal structure is tetragonal. At 600 K however, a difference in shape of diffraction spectra was also detected. At this temperature, the observed profile is much similar to the profile postulated by Vdovenko structure than that observed at 300 K. The same effect has been observed for measurements performed at higher temperatures. The very well observed effect was a rapid decrease in the intensity of reflections.

The structure analysis was performed for the tetragonal unit cell. The results of these calculations are presented in Tables 3 and 4. It was found that the angel of coil up of UBr_6^{-2} octahedron tends to zero as occurs for the cubic $Fm\bar{3}m$ structure. At 850 K, the values of unit cell constants seem to satisfy the relation $a_{tetr}\sqrt{2} = c_{tetr}$, suggesting that the tetragonal deformation was removed and the structure becomes a cubic structure reported by Vdovenko. The very high B factors could be interpreted as a result of high libration or rotation motions of the UBr_6^{-2} octahedrons around the central U ions. The fittings of the rest of neutron data were performed for the cubic structure.

Because the values of electric conductivity at temperatures close to the temperature of melting are high, one may expect disordering of rubidium sublattice. The Rb ions should be distributed randomly over other crystallographic positions. Among them, the stable positions are dodecahedral sites at the (8c) position, whereas quasi-stable octahedral sites are at the (4b) position. We decided to reduce the redistribution of Rb ions only to these positions. The final results are presented in Table 5.

It seemed that at 843 K, the transition occurred from the tetragonal to the cubic structure. This however stayed open the question of what was the source of effect observed on the DTA curve at 960 K. It is also seen that the factors of agreements for measurements at 900 K and 940 K were high, suggesting that the structure of the phase at the temperature region

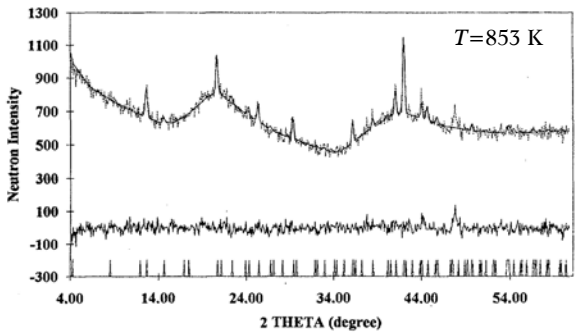

Fig. 8. Observed (points) and calculated (lines) neutron diffraction patterns of Rb_2UBr_6 (polycrystalline sample) obtained at 853 K on the NPD diffractometer. The curves at the bottom of diagrams show the difference $I_{obs} - I_{calc}$. The peak positions are marked by vertical lines. The non- linear background is due to the quartz container. The additional peak forbidden in the cubic K_2PtCl_6 type of structure and tetragonal structure of Rb_2UBr_6 is marked by arrow.

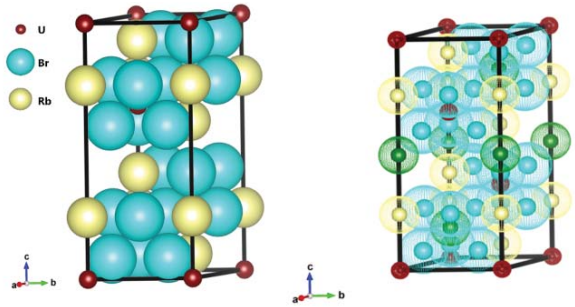

a b

Fig. 9. (a) The structure of Rb_2UBr_6 at 853 K. (b) The possible patches of conductivity are shown by thick lines. The Rb ions (yellow) residing temporary on the octahedral sites (green) create free holes inside the Rb sublattice, allowing the hopping process to occur between dodecahedral sites throughout the planar square sites.

846–960 K may be different. Hence, we decided to repeat the measurement at 850 K on the NPD diffractometer with a high instrumental resolution.

The NPD instrument was a high-resolution powder diffractometer. During our measurements, it used 10 ^{3}He detectors (separation 3.12°) with high-resolution (10'), Gd-coated mylar collimators. A Cu (220) double monochromator with an incident neutron wavelength of 1.470(1) Å was used throughout the experiment. Diffraction data were collected in 2Φ steps of 0.08° over the range of 4–137°. The measurements were performed at 850 K. The neutron diagram is shown in Fig. 8.

The high instrument resolution allowed precisely determination of position of diffraction lines. The obtained neutron diagram could not be indexed in a cubic system. The set of reflections however could be successfully indexed in the trigonal system with the unit cell constants: $a_{tri} = b_{tri} = 8.215$ and $c_{tri} = 20.10$ Å. They are related to the pseudo-cubic lattice by $a_{tri} \approx a_{cub}/\sqrt{2}$ and $c_{tri} \approx a_{cub}\sqrt{3}$. The trigonal unit cell may be derived from a cubic one as is shown in Fig. 9. The lack of any relations between hkl-type indexes and the transformations between cubic and trigonal structures assigned the trigonal structure to the $P\bar{3}ml$ space group.

The Rietveld profile refinement yields the atomic coordinates as shown in Table 6. These calculations were performed with the assumption that Rb ions may be distributed between dodecahedral and octahedral positions. The calculations were performed using anisotropic Debye–Waller factors. The view of structure is shown in Fig. 9.

Discussion and conclusions

The results of our investigations may be summarized as shown in Table 7. All observed structures could be treated as a deformed structure of K_2PtCl_6 type. The respective relations are shown in Fig. 10.

The sublattice of Br anions creates octahedral and dodecahedral environment of U^{+4} and Rb^{+1} ions, respectively. At low temperatures, dodecahedron sites are fully occupied by the Rb ions whereas uranium ions occupy octahedral positions partially.

The existence of phase transitions and rearrangement of Br positions in the temperature range

Table 6. Rb_2UBr_6 at T = 853 K, space group $P\bar{3}ml$, unit cell constant: a = b = 8.220(7), c = 20.100(5) Å

Name	Position	x	y	z	B	Occurence
Br_1	6i	–0.153(6)	0.153(6)	0.075(4)	—	1
Br_2	6i	–0.153(6)	0.153(6)	0.595(3)	—	1
Br_3	6i	1/2	0	0.242(2)	—	1
U_1	1a	0	0	0	24(4)	1
U_2	2d	1/3	2/3	0.3333	24(4)	1
Rb_1	2c	0	0	0.242(2)	28(6)	0.88(4)
Rb_2	2d	1/3	2/3	0.595(3)	28(6)	0.88(4)
Rb_3	2d	1/3	2/3	0.075(4)	28(6)	0.88(4)
Rb_4	1b	0	0	1/2	28(6)	0.24(2)
Rb_5	2d	2/3	1/3	0.16666	28(6)	0.24(2)

The anisotropic Debye–Waller factors (β*1E04)

Name	β_{11}	β_{22}	β_{33}	β_{12}	β_{13}	β_{23}
Br	4731 ± 414	10 321 ± 960	349 ± 30	5083 ± 493	1574 ± 154	964 ± 162

Reliability factors:
Least-squares refinement – Rp: 3.2, Rwp: 4.1, Rexp: 4.0, χ^2: 1.1.
Conventional Rietveld R-factors – Rp: 161, Rwp: 59, Rexp: 57, χ^2: 1.1.

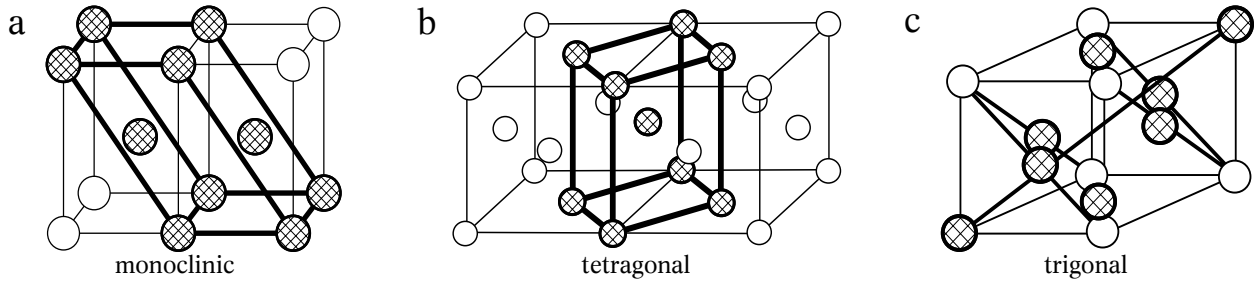

Fig. 10. (a) Transition from the pseudo-tetragonal to monoclinic unit cell appropriate to the P21/c space group. (b) Relation between the pseudo-cubic and tetragonal unit cells. (c) Relation between trigonal and cubic unit cells. For the sake of clarity, only U ions are shown.

Table 7. Compound Rb_2UBr_6

Phase	Temperature [K]	Space group	Lattice constants [Å]	Deviation
Monoclinic	4.2	P21/c	a = 7.637, b = 7.767, c = 13.232, β = 124.61°	
Tetragonal	300	P4/mnc	a = b = 7.745, c = 11.064	$D = \left(a\sqrt{2-c}\right)/c * 100\%$ $D = 1\%$
Tetragonal	600	P4/mnc tends to cubic $Fm\bar{3}m$	a = b = 7.96, c = 11.15	$D = \left(a\sqrt{2-c}\right)/c * 100\%$ $D = -0.96\%$
Tetragonal or cubic	850	P4/mnc tends to cubic $Fm\bar{3}m$	a = b = 8.15, c = 11.54	$D = \left(a\sqrt{2-c}\right)/c * 100\%$ $D = 0.12\%$
Trigonal	853	$P\bar{3}ml$	a = 8.215, c = 20.10	$D = \left(a\sqrt{2} - \left(\frac{c}{\sqrt{3}}\right)\right)\Big/\left(\frac{c}{\sqrt{3}}\right) * 100\%$ $D = 0.17\%$
Unknown	>960	not identified	for cubic system a = 11.92	

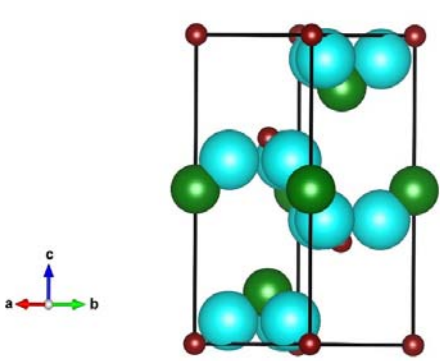

Fig. 11. The Rb and U ions residing on the octahedral sites. For the sake of clarity, some of Br ions are shown.

300–600 K suggest that the Rb_2UBr_6 structure can be easy locally deformed. Such an effect seems to be important for explanation of mechanism of ionic conductivity.

The conductivity is caused by the hopping process of Rb ions. It should occur between neighbour, dodecahedral sites throughout the quadratic walls of dodecahedrons. However, at low temperatures, all these sites are occupied and the process of hopping is forbidden. Therefore, in order to create free holes for the hopping process between dodecahedral sites, the Rb ions must reside in temporary octahedral interstices formed by six Br ions (cf. Fig. 9). There the problem appears. The large dimensions of Rb ions seem to prevent the octahedral position to be occupied (cf. Fig. 11). Therefore, a high temperature and the ability of the structure to occur local deformations are necessary for the occurrence of a high value of ionic conductivity.

The other explanation of ionic conductivity phenomena assumes the lack of stoichiometry. The excess of U^{+4} ions redistributed randomly over available octahedral sites yields "holes" in the rubidium sublattice, allowing the hopping process to occur.

The observed effect of ionic conductivity appears rapidly from 740 K [11]. It corresponds with a smoothly removal of tetragonal deformation and a high arising of Debye factors of Br ions. It increases rapidly when its temperature approaches to the trigonal phase transition. The temperature dependence of the conductivity does not indicate any abrupt increase in characteristic for a superionic phase. The structures observed at 853 K and 960 K confirm also that this compound reaches the melting point without passing through the superionic phase. It is worth to point out that together with Na_2UBr_6 (where superionic stay was observed), the value of entropy of melting is small, close to 13 kJ/mol*K [11]. This may be related to the high-temperature structures of both compounds. The small entropy of melting together with neutron investigations shows that below the melting point, the structures consist of rotated UBr_6^{-2} octahedrons.

Acknowledgment. The structural drawings were made using free VESTA computer program.

ORCID

Krzysztof Małetka http://orcid.org/0000-0002-5059-1481
Włodzimierz Szczepaniak http://orcid.org/0000-0003-4642-8128
Monika Zabłocka-Malicka http://orcid.org/0000-0003-2289-4706

References

1. Vdovenko, V. M., Kozhina, I. I., Suglobova, I. T., & Chirkst, D. E. (1973). Kompleksoobrazovane v sistemach galgenid urana – galgenid scelocnogo metalla. Polucenia i struktura Rb_2UBr_6 i Cs_2UBr_6. *Radiochimija*, *15*, 54–57.
2. Bendall, P. J., Fitch, A. N., & Fender, B. E. F. (1983). The structure of sodium hexachlorouranate(IV) and lithium hexachlorouranate(IV) from multiphase powder neutron profile refinement. *J. Appl. Cryst.*, *16*, 164–170. DOI: 10.1107/S0021889883010201.
3. Hewat, A. W., Taylor, J. C., Gaune-Escard, M., Bros, J. P., Szczepaniak, W., & Bogacz, A. (1984). Structural transitions and ionic conduction in Na_2UBr_6. *J. Phys. C-Solid State Phys.*, *17*, 4587–4600. DOI: 10.1088/0022-3719/17/26/009.
4. Małetka, K., Murasik, A., Fischer, P., & Szczepaniak, W. (1992). Structure analysis of Na_2UI_6 by neutron powder diffraction. *J. Appl. Cryst.*, *25*, 1–5. DOI: 10.1107/S0021889891007264.
5. Małetka, K., Murasik, A., Rundlöf, H., Tellgren, R., & Szczepaniak, W. (1995). High temperature phase transition in Na_2UI_6 by neutron powder diffraction. *Solid State Ion.*, *76*, 115–120. DOI: 10.1016/0167-2738(94)00198-2.
6. Małetka, K., Ressouche, E., Szczepaniak, W., Rycerz, L., & Murasik, A. (1996). Neutron diffraction studies of Me2UX6 ionic conductors. *Mater. Sci. Forum*, *228/231*, 711–716. https://www.scientific.net/MSF.228-231.711.
7. Małetka, K., Rundlöf, H., Tellgren, R., Szczepaniak, W., & Rycerz, L. (1996). Neutron diffraction and electrical conductivity studies of Li_2UI_6 ionic conductor. *Solid State Ion.*, *90*, 67–74. DOI: 10.1016/S0167-2738(96)00377-3.
8. Małetka, K., Ressouche, E., Tellgren, R., Rundlöf, H., Delaplane, R., Szczepaniak, W., & Malicka-Zabłocka, M. (1998). Phase transition in Li_2UBr_6 ionic conductor by neutron powder diffraction. *Solid State Ion.*, *106*, 55–69. DOI: 10.1016/S0167-2738(97)00480-3.
9. Małetka, K., Murasik, A., Zabłocka-Malicka, M., Szczepaniak, W., & Rycerz, L. (1997). Possibilities of ionic transport in uranium Li_2UX_6 and Na_2UX_6 (X=Cl,Br,I) solid electrolytes. In Proceedings of the 1st Conference on Ionic Liquids and Solid Electrolytes, June 12–14, 1997, Szklarska Poręba, Poland.
10. Szczepaniak, W. (1977). *Przemiany fazowe sześciobromo- i sześciojodouranianów(IV) litowców*. Unpublished Ph. D. Thesis, Politechnika Wrocławska. Wrocław, Poland.
11. Szczepaniak, W. (1990). *Heksabromo- i heksajodouraniany(IV) litowców jako stałe elektrolity*. Prace Naukowe Instytutu Chemii Nieorganicznej i Metalurgii Pierwiastków Rzadkich Politechniki Wrocławskiej. Monografie (Scientific Papers of the Institute of Inorganic Chemistry and Metallurgy of Rare Elements of the Technical University of Wrocław), No. 62. Wrocław: Oficyna Politechniki Wrocławskiej.
12. Gaune-Escard, M., Fouque, Y., Bross, J. P., Wiśniowski, M., & Bogacz Ber, A. (1989). Li_2UCl_6, Na_2UCl_6 and Cs_2UCl_6 compounds: Enthalpies of phase transitions and electrical conductivity in the solid and liquid states. Bunsenges. *Phys. Chem.*, *93*, 128–135. DOI: 10.1002/bbpc.19890930206.
13. Szczepaniak, W., & Bogacz, A. (1978). Novel alkali metal hexabromo- and hexaiodouranates(IV). *Mater. Sci.*, *4*(3), 117–120.
14. Małetka, K., Ressouche, E., Rundlöf, H., Tellgren, R., Delaplane, R., Szczepaniak, W., Rycerz, L., & Zabłocka-Malicka, M. (1997). *Phase transitions in Rb_2UBr_6 observed by neutron powder diffraction*. Świerk: Institute of Atomic Energy. (Internal report).
15. Rodriguez-Carvajal, J. (1990). FULLPROF: A Program for Rietveld Refinement and Pattem Matching Analysis. In Abstracts of the Satellite Meeting of the XV Congress of the Union Crystallography, Toulouse, France, 16–19 July 1990, p. 127.